Supplemental Information (SI)

Supplemental Figures

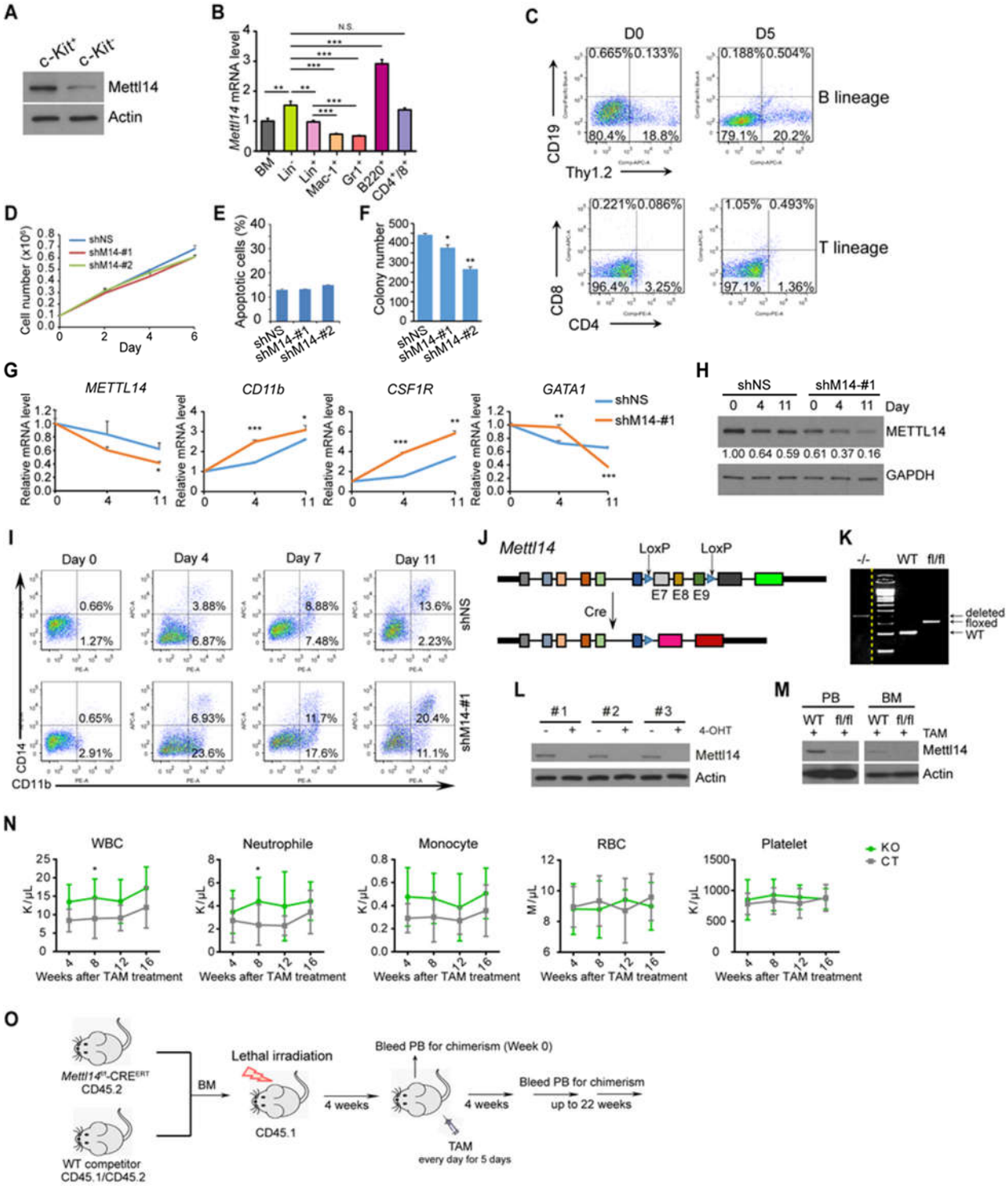

Figure S1 (related to Figure 1). *METTL14* in normal hematopoiesis.

(A) Western blot showing reduction of Mettl14 protein level in c-Kit$^-$ vs. c-Kit$^+$ populations in BM of CD45.2 mice.

(B) Relative expression levels of *Mettl14* in whole BM (set as 1) and different sub-populations of BM cells from wildtype B6.SJL mice as detected by qPCR.

(C) Flow cytometric analysis showing no induction of B lineage or T lineage cells during OP9 co-culture of Lin$^-$ HSPCs from BM of wildtype mice.

(D-F) Effects of METTL14 knockdown on normal CD34$^+$ HSPCs. Cord blood CD34$^+$ cells were transduced with shRNAs targeting METTL14 or scramble shRNA (shNS) and examined for cell proliferation (D), apoptosis (E), or colony-forming ability in H4434 methylcellulose-based medium (F).

(G) qPCR analysis of expression changes of *METTL14*, *CD11b*, *CSF1R*, and *GATA1* during differentiation in the control (shNS) and *METTL14*-depleted (shM14-#1) groups. Note that the CD34$^+$ HSPCs used here was from a different donor than that used for Figures 1G-I.

(H) Western blot showing expression changes of METTL14 in the control (shNS) and *METTL14*-depleted (shM14-#1) groups during differentiation. Signal of METTL14 was quantified and normalized to that of GAPDH.

(I) In vitro induced human CD34$^+$ cells were stained with CD11b and CD14 monocyte/macrophage surface markers at the indicated time points and subjected to flow cytometric analysis.

(J) Schematic diagram illustrating the LoxP/Cre-mediated deletion of Mettl14 in conditional knockout mice. E: exon. Note that changes in color of exons 10 and 11 indicate reading frame shift after Cre-mediated recombination.

(K) Genotyping of *Mettl14*$^{fl/fl}$-CRE^{ERT} mice before or after TAM treatment. A wild-type (WT) mouse was used as a control. Images were cropped from the same gel and merged as indicated by the dotted line.

(L) Western blot showing depletion of Mettl14 protein in BM cells from *Mettl14*$^{fl/fl}$-CRE^{ERT} mice after in vitro treatment with 4-OHT.

(M) Western blot showing depletion of Mettl14 protein in *Mettl14*$^{fl/fl}$-CRE^{ERT} mice after in vivo tamoxifen (TAM) treatment.

(N) Complete blood count of *Mettl14*$^{fl/fl}$-CRE^{ERT} mice treated with TAM or oil.

(O) Schematic outline of experiment strategy of in vivo competition assays.

Mean±SD values are shown for Figure S1B, D, E, F, G, and M. *, $p < 0.05$; **, $p < 0.01$; ***, $p < 0.001$; N.S., non-significant; t-test.

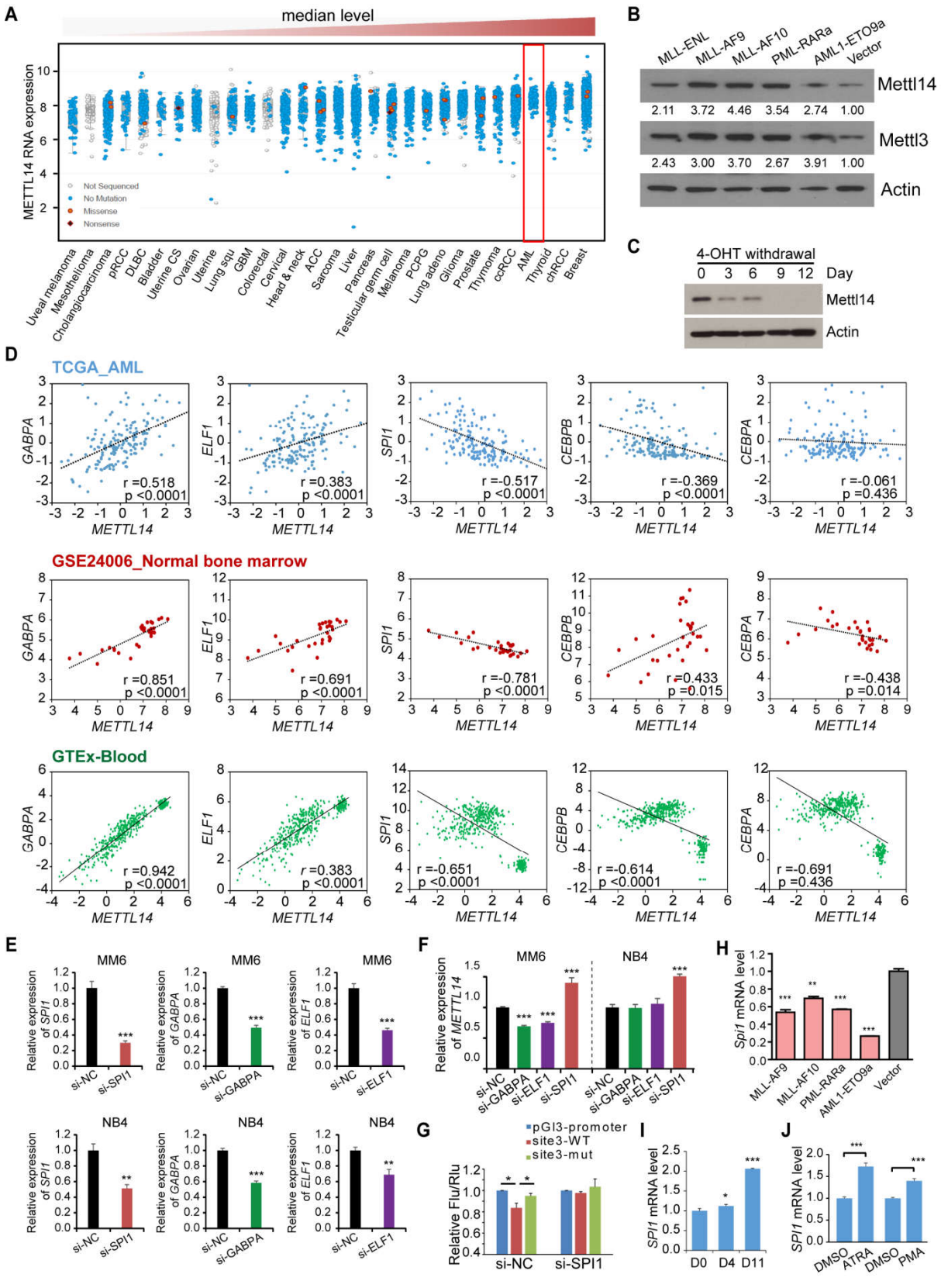
A
median level
METTL14 RNA expression
Not Sequenced
No Mutation
Missense
Nonsense
Uveal melanoma
Mesothelioma
Cholangiocarcinoma
pRCC
DLBC
Bladder
Uterine CS
Ovarian
Uterine
Lung squ
GBM
Colorectal
Cervical
Head & neck
ACC
Sarcoma
Liver
Pancreas
Testicular germ cell
Melanoma
PCPG
Lung adeno
Glioma
Prostate
Thymoma
ccRCC
AML
Thyroid
chRCC
Breast
B
MLL-ENL
MLL-AF9
MLL-AF10
PML-RARa
AML1-ETO9a
Vector
Mettl14
2.11 3.72 4.46 3.54 2.74 1.00
Mettl3
2.43 3.00 3.70 2.67 3.91 1.00
Actin
C
4-OHT withdrawal
0 3 6 9 12 Day
Mettl14
Actin
D
TCGA_AML
GABPA
ELF1
SPI1
CEBPB
CEBPA
METTL14
r =0.518 p <0.0001
r =0.383 p <0.0001
r =-0.517 p <0.0001
r =-0.369 p <0.0001
r =-0.061 p =0.436
GSE24006_Normal bone marrow
r =0.851 p <0.0001
r =0.691 p <0.0001
r =-0.781 p <0.0001
r =0.433 p =0.015
r =-0.438 p =0.014
GTEx-Blood
r =0.942 p <0.0001
r =0.383 p <0.0001
r =-0.651 p <0.0001
r =-0.614 p <0.0001
r =-0.691 p =0.436
E
MM6
NB4
Relative expression of SPI1
Relative expression of GABPA
Relative expression of ELF1
si-NC
si-SPI1
si-GABPA
si-ELF1
F
MM6
NB4
Relative expression of METTL14
si-NC
si-GABPA
si-ELF1
si-SPI1
G
pGl3-promoter
site3-WT
site3-mut
Relative Flu/Rlu
si-NC
si-SPI1
H
Spi1 mRNA level
MLL-AF9
MLL-AF10
PML-RARa
AML1-ETO9a
Vector
I
SPI1 mRNA level
D0
D4
D11
J
SPI1 mRNA level
DMSO
ATRA
DMSO
PMA

Figure S2 (related to Figure 2). *METTL14* is directly regulated by SPI1.

(A) Expression of *METTL14* in various types of cancer as adopted from cBioPortal for Cancer Genomics (http://www.cbioportal.org/). pRCC, Papillary Renal Cell Carcinoma; DLBC, Diffuse Large B-cell Lymphoma; GBM, Glioblastoma Multiforme; ACC, Adrenocortical Carcinoma; PCPG, Pheochromocytoma and Paraganglioma; ccRCC, Renal Clear Cell Carcinoma; chRCC, Chromophobe Renal Rell Rarcinoma.

(B) Mouse HSPCs were transduced with various fusion genes and seeded for CFA assays. Cells from 2nd round of plating were harvested and subjected to western blot for Mettl14 protein expression.

(C) Western blot showing a gradual decrease of Mettl14 protein level in MLL-ENL-ERtm cells after withdrawal of 4-OHT.

(D) Pearson correlation of hematopoietic transcription factors (TFs) with *METTL14* in expression in AML samples from TCGA, as well as normal BM samples from GSE24006 and blood tissues from the Genotype-Tissue Expression Project (GTEx).

(E) qPCR showing knockdown efficiency of siRNA pools targeting *SPI1*, *GABPA*, or *ELF1* in MM6 and NB4 cells 24 hours after electroporation.

(F) qPCR showing effect of silencing of *GABPA*, *ELF1*, or SPI1 on *METTL14* expression in MM6 and NB4 cells 24 hours after electroporation.

(G) Dual luciferase reporter assays. HEK293T cells were co-transfected with pGl3-promoter-based vector and si-NC/si-SPI1 siRNA together with pRL-TK plasmid. Cells were harvested 40 hours later for dual luciferase assays.

(H) Expression of *Spi1* mRNA in CFA cells shown in Figure 2C.

(I) Gradual increase of *SPI1* mRNA level during M-CSF-induced differentiation of human $CD34^+$ HSPCs in vitro as shown by qPCR.

(J) Expression change of *SPI1* in NB4 cells after treatment with 500 nM ATRA for 72 hours or with 0.5 ng/mL PMA for 48 hours as compared to the corresponding DMSO-treated cells.

Mean±SD values are shown for Figures S2E-J. *, $p < 0.05$; **, $p < 0.01$; ***, $p < 0.001$; t-test.

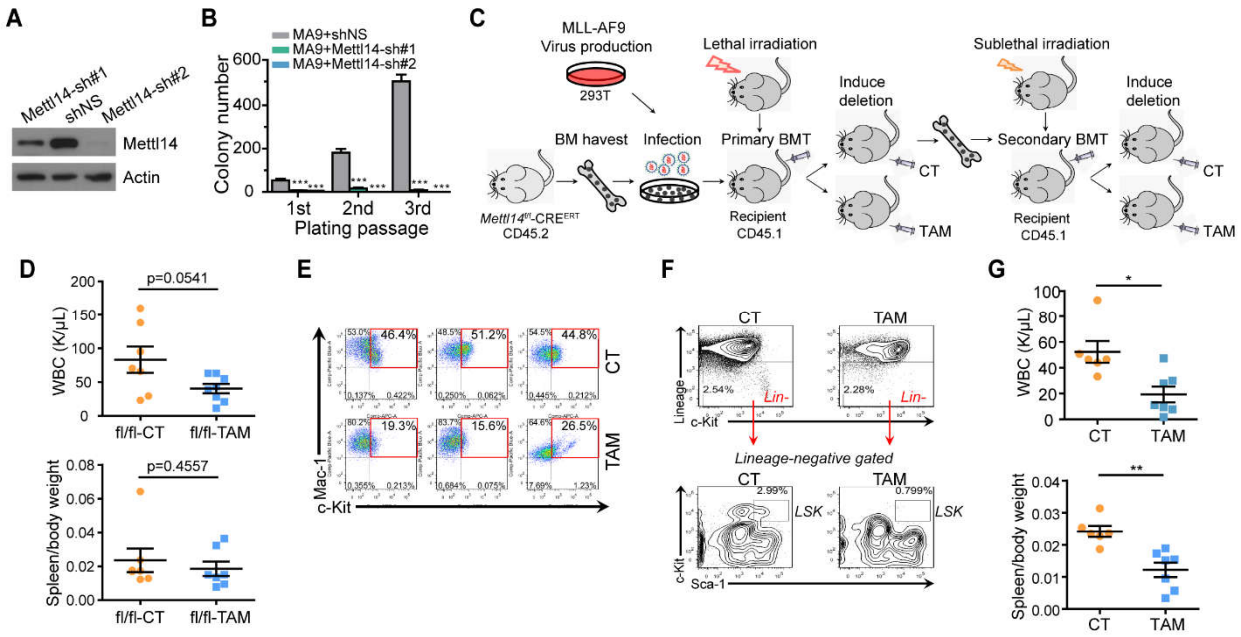

Figure S3 (related to Figure 3). Role of METTL14 in leukemogenesis.

(A) Western blot showing the knockdown efficiency of two individual shRNAs targeting mouse *Mettl14* in mouse embryonic stem cells (mES).

(B) Knockdown of *Mettl14* remarkably impaired in vitro cell transformation mediated by MLL-AF9. Wildtype mice HSPCs (BM progenitor cells) were transduced with MSCVneo-MLL-AF9 along with shNS, Mettl14-sh#1, or Mettl14-sh#2, and seeded for CFA assays.

(C) Schematic outline of experiment strategy of primary and secondary bone marrow transplantation (BMT) using MLL-AF9 leukemic cells.

(D) White blood cell (WBC) counts and spleen weight index of primary BMT recipient mice at the end point.

(E) Flow cytometric analysis showing reduction of Mac-1^{+}/c-Kit^{+} population in BM of primary BMT recipient mice treated with tamoxifen (TAM) compared to those treated with vehicle control (CT). Three mice from each group were analyzed.

(F) Schematic diagram showing gating of Lin^- and LSK populations in BM of primary fl/fl BMT mice.

(G) WBC counts and spleen weight index of secondary BMT recipient mice at the end point.

Mean±SD values are shown for Figures S3B, D and G. *, $p < 0.05$;**, $p < 0.01$; ***, $p < 0.001$; t-test.

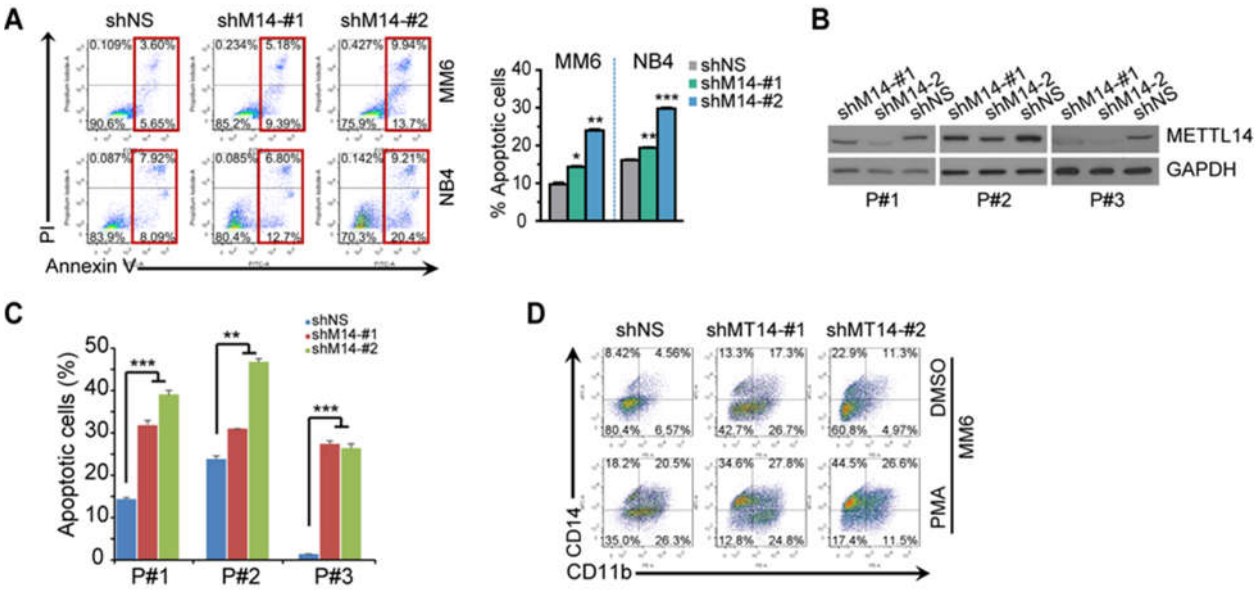

Figure S4 (related to Figure 4). METTL14 inhibits apoptosis and blocks myeloid differentiation in human AML cells.

(A) Knockdown of *METTL14* induces cell apoptosis. MM6 and NB4 AML cells were transduced with control (shNS) or *METTL14* (shM14-#1 and shM14-#2) shRNAs and subjected to flow cytometric analysis after staining with FITC-Annexin V and propidium iodide (PI). Percentages of apoptotic cells including early (Annexin V^+PI^-) and late apoptotic/necrotic (Annexin V^+PI^+) cells were shown as histograms on right.

(B) Western blot showing reduction of METTL14 in leukemia blasts from three AML patients by transduction of shRNAs targeting METTL14.

(C) Apoptosis assays of primary AML cells transduced with shRNAs targeting METTL14.

(D) MM6 cells with or without *METTL14* knockdown were treated with DMSO or PMA (1 ng/mL) for 24 hours and subjected to flow cytometric analysis.

Mean±SD values are shown for Figure S4A (right panel), and C. *, $p < 0.05$;**, $p < 0.01$; ***, $p < 0.001$; t-test.

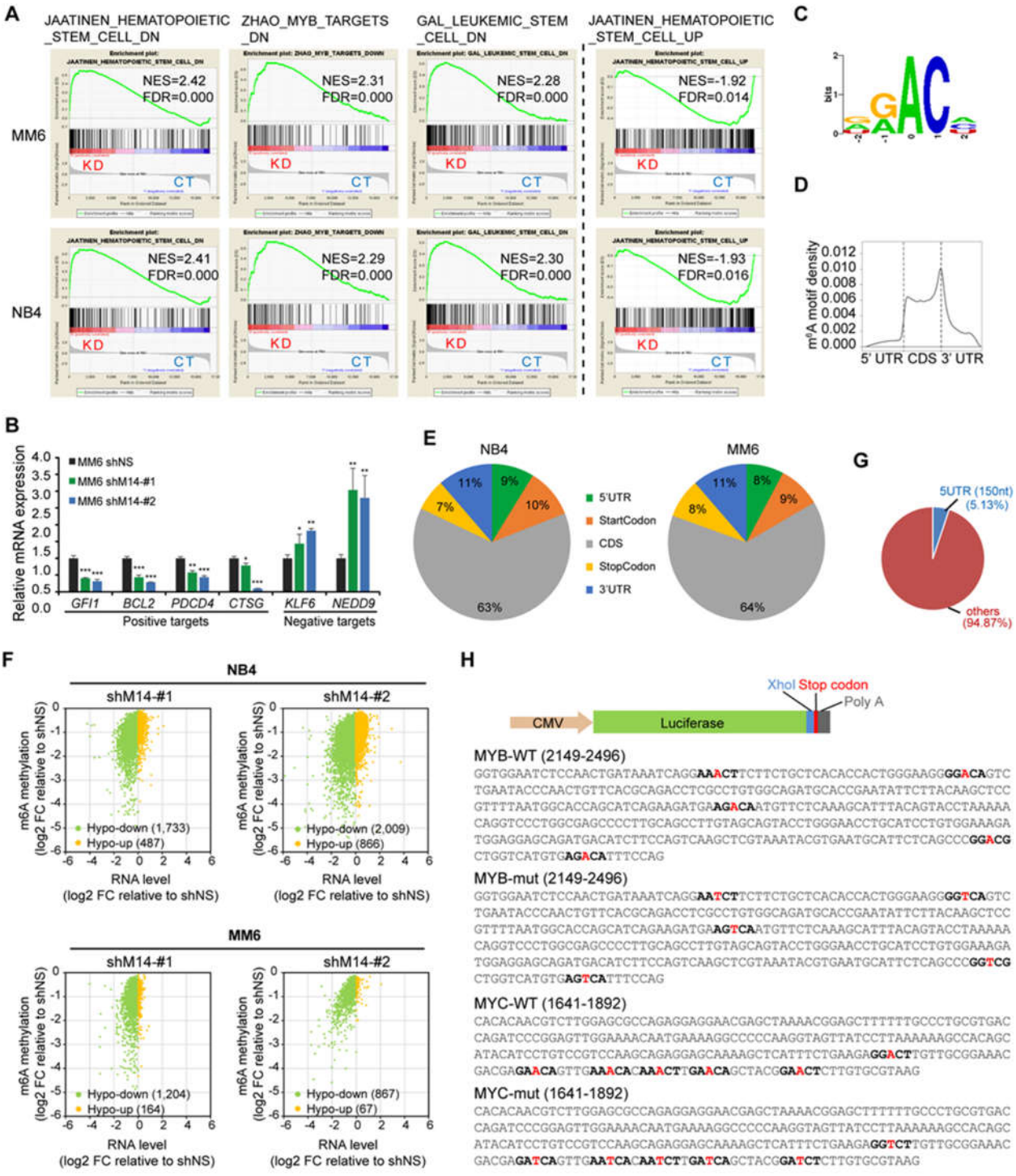

Figure S5 (related to Figure 5). Genome-wide identification of METTL14 targets.

(A) Gene set enrichment analysis (GSEA) (Subramanian et al., 2005) in MM6 and NB4 cells. Representative gene sets that are significantly enriched (p<0.0001 and FDR<0.05) in *METTL14*

knockdown samples (left panel) or control samples (right panel) were shown. KD, *METTL14* knockdown; CT, control; NES, normalized enrichment score; FDR, false discovery rate.

(B) qPCR showing expression changes of positive and negative targets of MYB in MM6 cells with or without *METTL14* knockdown.

(C) The predominant consensus motif DRACH ([G/A/U] [G/A] m^6AC [U/A/C]) detected by HOMER in m^6A-seq.

(D) The density distribution of m^6A peaks across the length of mRNA transcripts. Each region of 5' untranslated region (5'UTR), coding region (CDS), and 3' untranslated region (3'UTR) was split into 100 segments, and the percentage of m^6A peaks that fall within each segment was determined.

(E) The proportion of m^6A peak distribution in the 5'UTR, start codon, CDS, stop codon or 3'UTR region across the entire set of mRNA transcripts.

(F) Plots showing expression changes of transcripts with decreased m^6A abundance (m^6A-hypo; diff p <0. 01) upon *METTL14* knockdown in *METTL14* silenced (shM14-#1 and shM14-#2) cells relative to control cells. Note that the fold changes (FC) were log2 transformed. Numbers of hypo genes with reduced mRNA level (hypo-down) and increased mRNA level (hypo-up) were shown. diff p indicates whether the difference of a methylation site between the two experimental conditions tested is significant.

(G) Pie chart shows MM6-shM14-#2 cells as a representative the percentages of hypo-peaks located within the first 150 nt of 5' UTR as well as that in other regions (including the rest of 5'UTR, CDS, and 3'UTR).

(H) Construction of luciferase reporter vectors. Synthesized wildtype (WT) or mutant (mut) 3' coding sequences of *MYB* or *MYC* were inserted into the XhoI site right before the stop codon of

the luciferase reporter. The positions of *MYB* and *MYC* sequences used relative to their transcription start sites were shown. Putative m^6A consensuses were in bold while the mutation sites in red.

Mean±SD values are shown for Figure S5B. *, $p < 0.05$; **, $p < 0.01$; ***, $p < 0.001$; t-test.

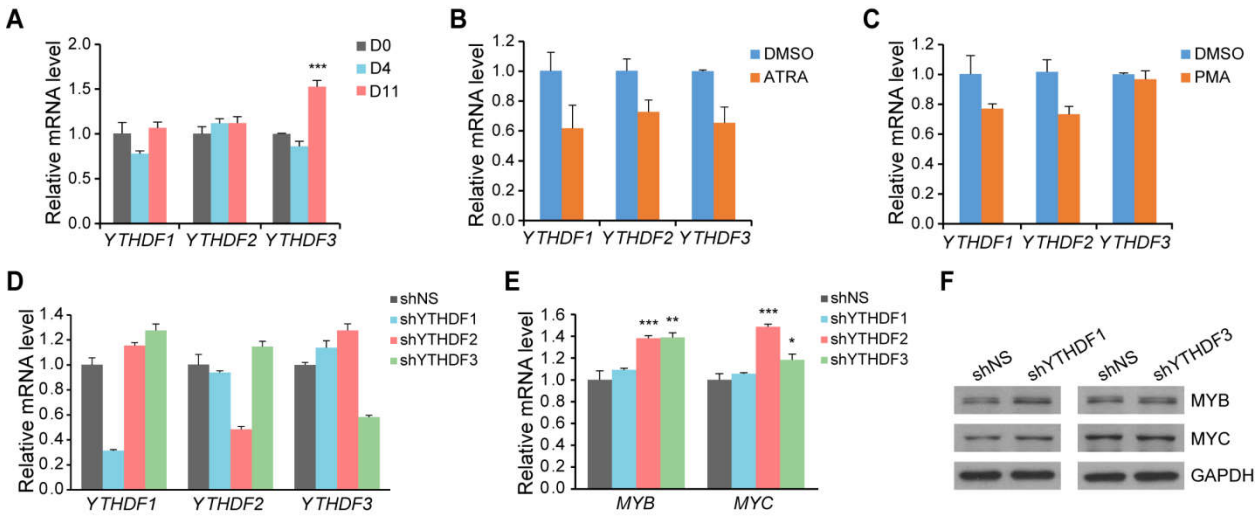

Figure S6 (related to Figure 6). YTHDF family proteins are not responsible for regulation of *MYB* and *MYC* by METTL14.

(A) Expression changes of YTHDF family members during M-CSF-induced differentiation of human $CD34^+$ HSPCs in vitro as shown by qPCR.

(B,C) Expression of YTHDF family members in NB4 cells after treatment with 500 nM ATRA for 72 hours (B) or 0.5 ng/mL PMA for 48 hours (C) as compared to DMSO-treated cells as detected by qPCR.

(D) qPCR showing specific knockdown of YTHDF family members by individual shRNA in MM6 cells.

(E) qPCR showing changes of *MYB* and *MYC* mRNA levels in MM6 cells transduced with shRNAs targeting YTHDF family members.

(F) Western blot showing expression of MYB and MYC proteins in MM6 cells with or without YTHDF1/3 knockdown.

Mean±SD values are shown for Figure S6A-E. *, $p < 0.05$; **, $p < 0.01$; t-test.

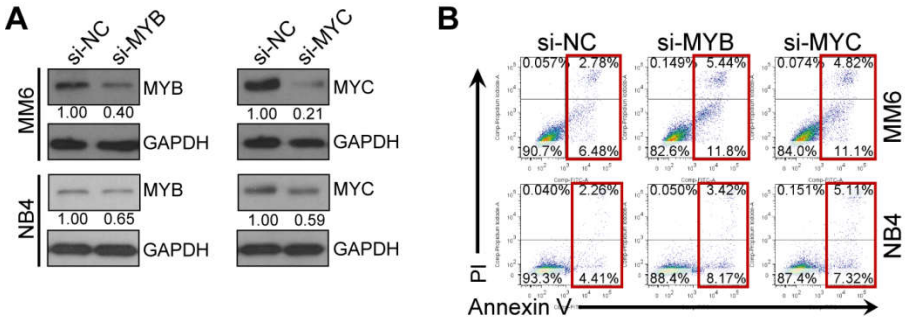

Figure S7 (related to Figure 7). Silencing of *MYB* and *MYC* induces cell apoptosis.

(A) Western blot showing knockdown efficiency of *MYB* and *MYC* by gene specific siRNA pools. MM6 and NB4 cells were transfected with scramble siRNA (si-NC) or siRNA pools targeting *MYB* (si-MYB) or *MYC* (si-MYC) via electroporation. Forty-eight hours later, cells were collected for western blot analysis.

(B) MM6 and NB4 cells were stained with FITC-Annexin V and propidium iodide (PI) 48 hours later after transfection and subjected to flow cytometric analysis.

Supplemental Tables

Table S1 (related to STAR Methods). List of oligonucleotides

Name	Sequence	Note
METTL14-qPCR-F	TTTCTCTGGTGTGGTTCTGG	qPCR of human genes
METTL14-qPCR-R	AAGTCTTAGTCTTCCCAGGATTG	
SPI1-qPCR-F	AGTTCCTGTTGGACCTGCTC	
SPI1-qPCR-R	AACTGGAAGGTGCCCTTGTC	
GABPA-qPCR-F	AGAACAAGTGACAAGATGGGC	
GABPA-qPCR-R	TCGGTCATGCTGAATTCCTTC	
ELF1-qPCR-F	CATCACCAGAACAGCCTAAGAG	
ELF1-qPCR-R	TTGTGTTTCCCTTTCCATCTTTG	
MYB-qPCR-F	CAAGCTCCGTTTTAATGGCAC	
MYB-qPCR-R	ATCTTTCCACAGGATGCAGG	
MYC-qPCR-F	TTCGGGTAGTGGAAAACCAG	
MYC-qPCR-R	AGTAGAAATACGGCTGCACC	
CD11b-qPCR-F	GTGGCAAGGAATGTATTTGAGTG	
CD11b-qPCR-R	CAGAGCCAGGTCATAAGTCAC	
CSF1R-qPCR-F	GGGAATCCCAGTGATAGAGCC	
CSF1R-qPCR-R	TTGGAAGGTAGCGTTGTTGGT	
GATA1-qPCR-F	AAGAAGCGCCTGATTGTC	
GATA1-qPCR-R	AGATGCCTTGCGGTTTC	
GFI1-qPCR-F	GTTTGAGGACTTCTGGAGGC	
GFI1-qPCR-R	AGTACGGTTTGAAAGGCAGG	
BCL2-qPCR-F	GTGGATGACTGAGTACCTGAAC	
BCL2-qPCR-R	GCCAGGAGAAATCAAACAGAGG	
PDCD4-qPCR-F	TGGGCCAGTTTATTGCTAGAG	
PDCD4-qPCR-R	ACGCTTTCCACCTTTAGACATAC	
CTSG-qPCR-F	TGGTGCGAGAAGACTTTGTG	
CTSG-qPCR-R	TGATTATATTGAGGGTGGCGG	
KLF6-qPCR-F	CTTTAACGGCTGCAGGAAAG	
KLF6-qPCR-R	GGAAGTGCCTGGTTAACTCATC	
NEDD9-qPCR-F	TGTAGGAAAACGGCTCAACC	
NEDD9-qPCR-R	CCCTGTGTTCTGCTCTATGAC	
GAPDH-qPCR-F	AATCCCATCACCATCTTCCAG	
GAPDH-qPCR-R	AAATGAGCCCCAGCCTTC	
ACTB-qPCR-F	CACTCTTCCAGCCTTCCTTC	
ACTB-qPCR-R	GTACAGGTCTTTGCGGATGT	
Mettl3-qPCR-F	ATCCAGGCCCATAAGAAACAG	qPCR of mouse genes
Mettl3-qPCR-R	CTATCACTACGGAAGGTTGGG	
Mettl14-qPCR-F	GGAGCGGCAGAAGTTACG	
Mettl14-qPCR-R	GCAGATGTATCATAGGAAGCCC	
Wtap-qPCR-F	TTTGGAGGGAAAGTACACAGATC	

Wtap-qPCR-R	TCCTGCTCTTTGGTTGCTAG	
Fto-qPCR-F	TCACAGCCTCGGTTTAGTTC	
Fto-qPCR-R	GCAGGATCAAAGGATTTCAACG	
Alkbh5-qPCR-F	AGTTCCAGTTCAAGCCCATC	
Alkbh5-qPCR-R	GGCGTTCCTTAATGTCCTGAG	
Spi1-qPCR-F	CCTCCATCGGATGACTTG	
Spi1-qPCR-R	GTGTGCGGAGAAATCCCA	
Myb-qPCR-F	TTTCAGTAACGGTGGTCCACTCT	
Myb-qPCR-R	TAAGCAGGAATCGGATGAATCTG	
Myc-qPCR-F	GCTGTTTGAAGGCTGGATTTC	
Myc-qPCR-R	GATGAAATAGGGCTGTACGGAG	
Gapdh-qPCR-F	CCTGCACCACCAACTGCTTA	
Gapdh-qPCR-R	TCATGAGCCCTTCCACAATG	
Actb-qPCR-F	AGAGGGAAATCGTGCGTGAC	
Actb-qPCR-R	CAATAGTGATGACCTGGCCGT	
MYB-m^{6}A-F	GCATTCTCAGCCCGGACG	m^{6}A-qPCR and CLIP-qPCR
MYB-m^{6}A-R	CACAACAAAAATAGGTTCTTCTCCC	
MYC-m^{6}A-F	GCATACATCCTGTCCGTCCA	
MYC-m^{6}A-R	GTCGTTTCCGCAACAAGTCC	
Myb-m^{6}A-F	CGTTCCCTATCCTGTCGCA	
Myb-m^{6}A-R	GCTCCTTTATTCGCTTTTCC	
Myc-m^{6}A-F	CAGATCAGCAACAACCGCAAGT	
Myc-m^{6}A-R	CTGGTCACGCAGGGCAAAA	
M14-site1-F	CCAGAGGGGAGGAATGCTA	ChIP-qPCR
M14-site1-R	GGTGTATGGAAGGTGATTGAGTT	
M14-site2-F	TGGAGGGCATTCTAGTAAGATGT	
M14-site2-R	ATCGCTTGAACTGGGGACG	
M14-site3-F	TGGAGGAGTCAGTCTCCAGG	
M14-site3-R	TTATGACAACATAAAGGCCACTAG	
M14-site4-F	TCCAGGCAGGAAAACAAAT	
M14-site4-R	CTGTTCCACCAGCTCAAGG	
M14-site5-F	TACACCAAGGGAACCTGCTA	
M14-site5-R	CTGGACGCTTGCTATGTGAC	
M14-site6-F	CAGACTCGGAAGAAAGGTTGG	
M14-site6-R	GAGGAGCTGTCGCCGTAAC	
M14-NC-F	GGGTAGATAAAGGAGAATAGAGCA	
M14-NC-R	GCCTGAAGAACATAAGCCAGTT	